1-1-1986

Chemical Applications of Scanning Tunneling Microscopy

Paul West

John Kramer

David V. Baxter
California Institute of Technology

Robert J. Cave
Harvey Mudd College

John D. Baldeschwieler
California Institute of Technology

Chemical applications of scanning tunneling microscopy

by Paul West
John Kramar
David V. Baxter
Robert J. Cave
John D. Baldeschwieler

The development of a scanning tunneling microscope at the California Institute of Technology is well under way. Electron tunneling has been demonstrated, and preliminary surface images of gold films have been obtained. Additional instrumental development is required to achieve the atomic resolution which is required for the study of chemical processes on surfaces. A theoretical model is also being developed for the study of tunneling of electrons from the probe to surfaces with molecular species adsorbed, and with atomic and molecular species intervening between the probe and the surface. These experimental tools and theoretical models, which are being developed concurrently, will be applied to the study of chemical systems and processes on surfaces. Some of the first molecular species for study will include benzene and pyridine on metal surfaces, and porphyrins and phthalocyanines on pyrolytic graphite. The applications that can be imagined for STM in surface chemistry are very broad, and the choice of additional systems for study will be based on the results of these initial experiments.

Introduction

A number of surface-sensitive probes have been introduced in the past twenty years which together are capable of determining chemical composition, surface structure for ordered simple surfaces, and surface electronic properties averaged over large areas of the surface. These techniques have greatly increased our understanding of surface phenomena. However, these methods usually do not provide an analysis on a local atomic level.

Within the past few years a new technique for surface studies has been introduced by Binnig et al. [2–9] which is capable of atomic resolution. This method involves positioning a probe a few angstroms from the surface of interest. A small potential is applied across the gap and the electron tunneling current is measured. The probing tip is then scanned across the surface in two dimensions while the distance between the tip and surface is adjusted to maintain a constant current. In this way the tip is made to follow the contours of the surface. The real space resolution obtained in this way is about 3 Å parallel to the surface and 0.1 Å in the surface normal. Binnig et al. [2–9] have called this instrument a scanning tunneling microscope (STM).

Although the main uses of the STM to date have been in elucidating surface structure [3, 6, 8], it is also possible to apply this technique to gain understanding of surface electronic properties and chemical composition. The unique ability of the STM to resolve both position and chemical identity in real space on an atomic level makes it ideally suited for the study of chemical processes on surfaces [10, 11]. The orientation of the molecules with respect to the underlying surface should be observable, as well as the structure of molecular species including reactants, products, and some of the reaction intermediates.

Project status

• *Instrumentation*

In order to achieve vacuum tunneling, a controllable vacuum gap must be maintained. Herein lie the major experimental constraints and difficulties of the STM. Mechanical isolation must be achieved which will allow extraneous vibrations to perturb the distance between the tip and the surface no more than 0.05 Å (to achieve 0.1 Å vertical resolution). Also, a method of controlling this distance and positioning the tip in the surface plane must be provided. For the highest resolution, the system must also be ultrahigh-vacuum (UHV) compatible.

The Caltech system uses a Varian FC-112-based vacuum system which includes a 200-liter-per-second triode ion pump and an auxiliary titanium sublimation pump. We employ the spring isolation system which was originated at IBM [4, 5]. The probe tip is positioned relative to the surface in two stages. For fine positioning, the tip is mounted on a piezoceramic assembly which can move the tip in the Cartesian coordinates. The fine-positioning assembly consists of two separate ceramics, one for surface plane (x and y) motion and another for surface normal (z) motion. For coarse motion, the fine-positioning assembly is mounted on a piezoceramic "louse." The sample to be studied is mounted on a macor block in front of the probing tip. The STM probing tips have been made by grinding 1-mm tungsten wire to a point. This gives an overall tip radius of about a micrometer, but smaller mini-tips are created by the rough grinding process [4].

• *Experimental results*

There are several modes of operation of the STM with which we have experimented. The simplest mode of operation is to study the dependence of tunneling current on the distance between the probe and the surface. This is done by maintaining a constant potential across the tunneling junction and decreasing the tunneling gap while monitoring the current. Plots of the logarithm of the current vs. the tip-to-surface distance (as computed from the piezoelectric coefficients of the ceramic, and the applied voltage) yield straight lines, as predicted from a simple one-dimensional square-barrier, stationary-state calculation. From the same calculation, the slope of the line should be equal to a fundamental constant times the square root of the work function. This is borne out in our data for a scan of this type using a tungsten tip ($\phi = 4.6$) and a gold surface ($\phi = 5.1$) which gives a work function of 5.2, which is reasonable considering the unprepared nature of the surfaces (**Figure 1**). One can envision a study of the change in work function of a surface as a function of the identity and surface coverage of adsorbates.

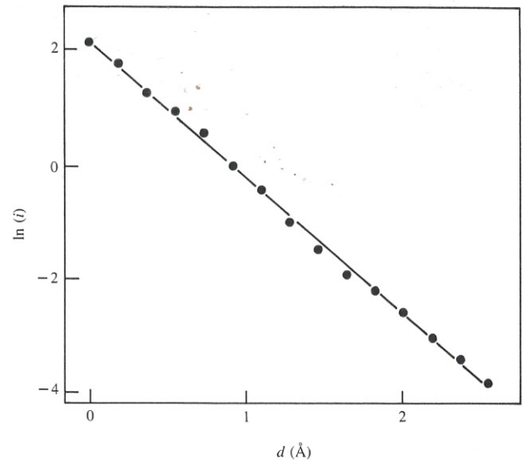

Figure 1

Plot of $\ln(i)$ vs. relative distance, d, for a tungsten tip and a gold foil surface. The work function determined from the slope of the line is 5.2 eV.

A somewhat more complex mode of operation is that used to study the voltage dependence of current at constant distance. In this experiment we first stabilize the position of the tip at a fixed distance from the surface by running the constant-current feedback at a given initial voltage. Initial voltages are typically 10 mV, and the distance is adjusted to maintain a constant current of 5 nA, which corresponds to 5–10 Å. The feedback loop is then disconnected, and the voltage is quickly ramped in a triangular pulse using a PAR potentiostat. The voltage pulse and the current response as amplified by the Keithley electrometer are both stored versus time on a Tektronix Model 5223 storage oscilloscope. **Figure 2** is a typical scan obtained by this mode of operation. The underlying structure observed in the current vs. voltage scans can be qualitatively explained in terms of a one-dimensional square barrier distorted by an applied voltage [12].

Three-dimensional surface scanning is the third mode of operation with which we have experimented. In this case, a constant potential (typically 10 mV) is applied across the tunneling junction. The distance between the probe and the surface is adjusted by means of the feedback loop, which maintains a constant tunneling current of typically 5 nA. The probe is moved across the surface by changing the potentials on the x and y piezoceramics, and the voltage applied to the z ceramic (as set by the feedback loop) is recorded as a function of x and y position.

Figure 3 is an example of surface scanning performed with our STM. The tip was a 1-mm tungsten wire ground to a point by a grinding wheel, and the substrate was a layer of

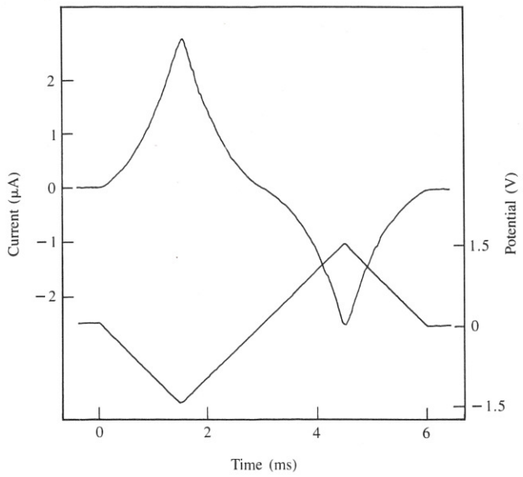

Figure 2

Plot of voltage applied across the tunneling gap and current observed vs. time at constant distance.

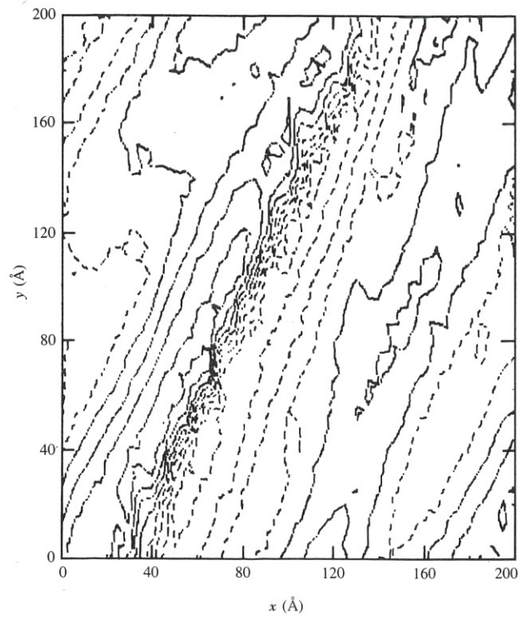

Figure 3

Contour plot of an STM scan of a 1000-Å thickness of gold vapor deposited on a glass slide. Solid lines represent positive contours, dotted lines negative contours. The vertical distance between the highest and lowest contour is about 160 Å.

gold vapor ~1000 Å thick deposited on a glass slide. The scan was made using the analog feedback loop, averaging together five passes over the surface. The origin of the ~160-Å step which runs through the center of the scan is unknown, although it is similar to early results reported by other groups for uncharacterized gold surfaces [13]. A subsequent scan on the 40 × 40-Å square nearest the labeled origin is shown in **Figure 4.** In this scan, part of the 160-Å step is also visible, indicating reproducibility of the scan.

Future studies

• *Experimental objectives*

There is still much to be done before the potential of the scanning tunneling microscope in studying chemical processes on surfaces can be fully realized.

Recently a new type of vibration isolation system has been developed by the researchers at IBM [14]. The basic mechanism employed is mass damping through elastomers. We are currently building a vibration isolation unit of this type and plan to add it to our existing system by simply placing it on the center stage of our current vibration isolation unit. It is hoped that the two types of vibrational isolation will be complimentary to each other, the spring damping being more effective for large-amplitude vibrations and the viton stainless-steel stack being more effective for the higher-frequency vibrations.

It will be advantageous in our work to be able to measure simultaneously a contour of constant electron density and the spatially resolved rate of decay of the surface wave function. In order to achieve this, some combination of constant-current scanning and distance-dependent-current scanning must be employed. We envision using a scheme similar to the design used by Elrod et al. [15] for accomplishing this.

A sample-preparation chamber equipped with an airlock has been designed for the microscope and is being built. The overall arrangement is to attach the sample-preparation chamber to the existing bell jar, separating the two by a gate valve. The airlock chamber is also isolated from the sample-preparation chamber by a gate valve and is located opposite the microscope chamber. A 30-inch-stroke translator (UHV Instruments Model 1000) which is used for moving samples among the three chambers is mounted on the opposite side of the airlock chamber. To introduce a new sample into the system, the airlock chamber is opened with both gate valves closed and the long-stroke translator fully retracted. Then the sample can be placed on the translator, the airlock chamber sealed and evacuated, and the gate valve into the sample-preparation chamber opened to allow the translator and sample access. Similarly, if any of the procedures used in sample preparation involve pressures and reagents which are not desired in the microscope, the microscope can be isolated by means of the gate valve between the two chambers for the duration of the procedure and subsequently opened to allow the translator access to the microscope. The sample-preparation chamber itself will be a standard surface-analysis system.

The sample-preparation chamber and sample-loading airlock will greatly enhance the versatility of our instrument. The sample-preparation chamber will provide a means of preparing well-characterized samples for microscope study. The airlock will allow the introduction of new substrates without the bakeout necessary when vacuum is broken. This addition should allow us to study many chemical systems with minimal downtime.

• *Theoretical considerations*

The theoretical component of our research is focused on assessing the changes in the tunneling current caused by variations in the size and structure of surface adsorbates. Our aim is to use theory as a means of qualitatively understanding how the physical properties of an adsorbate (e.g., ionization potential, electron affinity, atomic radius, etc.) might influence the tunneling current. Since the effects of such adsorbates can be assumed local, our calculations use clusters to model the surface and tip, and use *ab initio* electronic structure techniques to obtain the cluster wave functions. The calculations are being performed in association with the research group of W. A. Goddard III at Caltech. Such clusters have been used previously to model interactions of adsorbates with metal surfaces [16, 17].

Previous theoretical investigations of STM have been carried out by a number of groups which have examined idealized surfaces [18–21] and reconstructed surfaces of metals and semiconductors [22, 23], as well as the effects of single-atom adsorbates on the tunneling current density between two parallel plate electrodes [24]. By using time-dependent, first-order perturbation theory, the tunneling current between the surface and tip can be obtained approximately as [22, 23, 25].

$$I = \frac{2\pi e}{\hbar} \sum_{\mu,\nu} f(E_\mu)[1 - f(E_\nu + eV)]|T_{\mu\nu}|^2 \delta(E_\mu - E_\nu), \quad (1)$$

where $f(E_\mu)$ is the Fermi function for the surface, V is the applied voltage, and $T_{\mu\nu}$ is the electronic coupling matrix element between states ψ_μ and ψ_ν taken to be the surface and tip states, respectively. In the limits of low temperature and low applied voltage, Equation (1) reduces to [22, 23]

$$I = \frac{2\pi e^2 V}{\hbar} \sum_{\mu,\nu} |T_{\mu\nu}|^2 \delta(E_\mu - E_F)\delta(E_\nu - E_F). \quad (2)$$

It is seen that the tunneling current is directly related to the size of the electronic matrix element $T_{\mu\nu}$. The full expression for $T_{\mu\nu}$ is [26, 27]

$$T_{\mu\nu} = \frac{\langle\psi_\mu|H_{TOT}|\psi_\nu\rangle - S_{\nu\mu}\langle\psi_\nu|H_{TOT}|\psi_\nu\rangle}{1 - |S_{\mu\nu}|^2}. \quad (3)$$

Here ψ_μ and ψ_ν are assumed to be the full many-electron wave functions of the system with the "extra" electron bound to the surface and tip respectively. In practice ψ_μ and ψ_ν must be truncated. For example, when the nontransferring (or "core") electrons on the tip and surface are assumed to be unaffected by the presence or absence of the transferring electron, these core electrons can be neglected in ψ_μ and ψ_ν. Further, when the one-electron wave functions representing ψ_μ and ψ_ν are eigenfunctions of the surface and tip potentials respectively, $T_{\mu\nu}$ becomes

$$T_{\mu\nu} = \frac{\langle\psi_\mu|V_{tip}|\psi_\nu\rangle - S_{\nu\mu}\langle\psi_\nu|V_{tip}|\psi_\nu\rangle}{1 - |S_{\mu\nu}|^2}. \quad (4)$$

Since ψ_μ and ψ_ν decay exponentially with distance from their respective surfaces, the second term in the numerator of Equation (4) can be neglected, the denominator is essentially unity at large enough distances, and $T_{\mu\nu}$ becomes

$$T_{\mu\nu} = \langle\psi_\mu|V_{tip}|\psi_\nu\rangle. \quad (5)$$

The quantity in Equation (5) was evaluated by Tersoff and Hamann [22, 23] using the Bardeen expression [25] for the matrix element.

In our studies we have chosen to use *ab initio* electronic structure techniques to examine $T_{\mu\nu}$. The main advantage in using these methods is that they should afford a reasonably accurate description of the adsorbate-surface interaction.

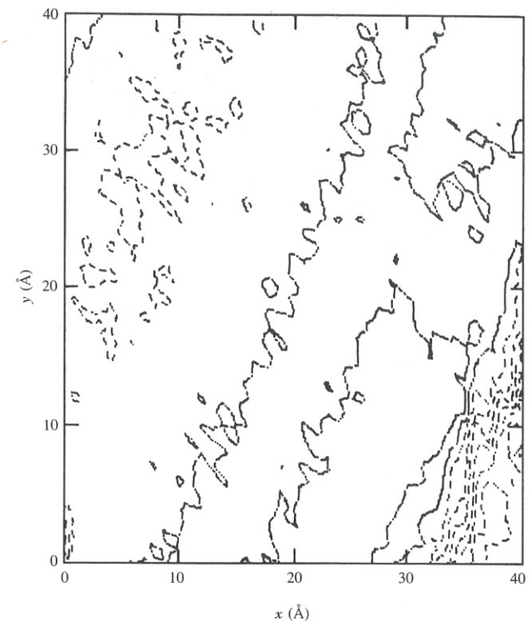

Figure 4

A subsequent scan of the surface shown in Figure 3, showing the 40 × 40-Å sector nearest the labeled origin. The vertical displacement from highest to lowest contour is about 40 Å.

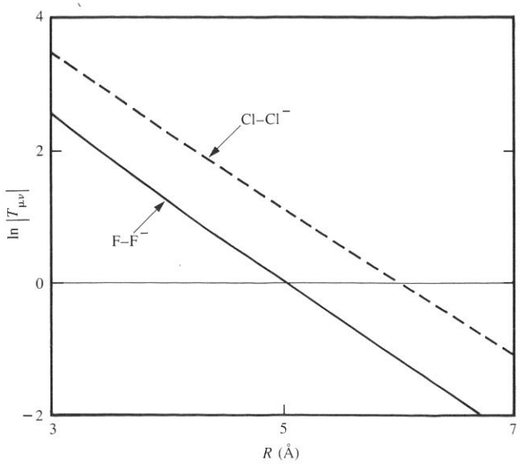

Figure 5

Plot of $\ln|T_{\mu\nu}|$ as a function of center-to-center separation distance for the atomic pairs $F–F^-$ and $Cl–Cl^-$. The values of $T_{\mu\nu}$ are in millihartrees, the separation distances in Å.

The truncation of ψ_μ and ψ_ν entails the limitation of the region of the surface and the tip to be considered, since two-dimensionally infinite slab calculations are currently unfeasible using *ab initio* methods, due to the excessive integral evaluation time which would be required. ψ_μ and ψ_ν then become the many-electron wave functions describing these fragments and no further approximations are made in the evaluation of Equation (3) for $T_{\mu\nu}$. Such electronic structure techniques have been applied previously to the study of charge-transfer reactions in aqueous solution [28–30], and efficient methods for the evaluation of $T_{\mu\nu}$ have been developed [28, 31].

There are certain disadvantages in using such techniques to characterize tunneling processes. First, the behavior of such wave functions is inaccurate at large distances from the atom of interest since they decay as $\exp(-\alpha r^2)$ rather than as $\exp(-\alpha r)$. This limits the range of distances over which our results will be valid. Since our main interest is in comparisons of the effects of a variety of adsorbates on $T_{\mu\nu}$ (and therefore, the tunneling current), these effects can be examined over distances where the basis set effects are not a problem, and then extrapolated to larger distances if desired.

A second difficulty in the use of *ab initio* methods lies in the utilization of cluster descriptions for the tip and surface. The effects of the electronic response of the clusters upon gain or loss of an electron will need to be examined. For example, in the actual system, the "fractional charge" lost or gained by any given atom at the surface or the tip upon electron transfer is infinitesimally small, whereas, in the cluster description, the fractional gain or loss of charge can approach unity as the cluster size shrinks. The remaining electronic charge will respond to this by changing shape, which can, in principle, affect $T_{\mu\nu}$.

Our initial aim is to characterize the energy dependence and orbital shape dependence of $T_{\mu\nu}$ in relatively simple systems. Therefore, we have calculated $T_{\mu\nu}$ as a function of distance for charge transfer between pairs of second- and third-row halide atoms, as well as pairs of alkaline-earth metals. From such results the effects of changes in ionization potential and atomic size can be examined, which should aid in interpreting results on more complex systems.

In **Figure 5**, results are shown for the tunneling matrix element as a function of distance in the systems $F–F^-$ and $Cl–Cl^-$. The wave functions were obtained at the Hartree-Fock level using standard basis sets [32]. The tunneling matrix element is seen to decay essentially exponentially with distance over the range of distances shown. Distances up to 10 Å were examined in the case of $F–Cl^-$ (not shown) and the decay of $\ln|T_{\mu\nu}|$ was also found to be basically linear. Essentially identical results were obtained for $T_{\mu\nu}$ beyond 4 Å using wave functions for each center obtained in the absence of the second atom, thus indicating that the interaction between the centers is small at these distances, as it should be.

Using Koopmann's theorem [33], an estimate of the ionization potential of a given orbital can be obtained from the Hartree-Fock orbital energy. For F^- our results yield 4.9 eV and for Cl^- they yield 4.0 eV. On this basis it is expected that the decay of $T_{\mu\nu}$ with distance should be somewhat greater when F^- is involved than when it is not. The results of Figure 5 bear this out but it is apparent that the difference in decay rate is, in any event, rather small.

It can also be seen from Figure 5 that the size of $T_{\mu\nu}$ can vary considerably at a given R as a function of the atoms involved in the transfer. This effect can be attributed to the difference in size of the 2p F orbitals and the 3p Cl orbitals, the latter having larger electron density at greater distances from the nucleus, thus increasing $T_{\mu\nu}$ at a given R relative to the fluorine case.

Results have also been obtained for transfers in the systems $Be–Be^+$ and $Mg–Mg^+$, and they are shown as functions of distance in **Figure 6**. The decay of $T_{\mu\nu}$ with distance is again seen to be essentially exponential with distance.

The effects of orbital shape on the lateral displacement behavior of $T_{\mu\nu}$ are examined in **Figure 7**. The orientations examined are shown in Figure 7(a). In Figure 7(b) the results labeled "Exact" are for calculations of $T_{\mu\nu}$ for $\Delta z = 5.5$ Å and δ varying from −2 Å to +2 Å. The results labeled "Estimated" correspond to an estimate of this variation based on the assumption that the decrease in $T_{\mu\nu}$ for nonzero δ is merely due to an increase in center-to-center separation distance, and calculated for increasing Δz along the $\delta = 0$ line. The additional decay in the former case can be attributed to the nonspherical shape of the fluorine 2p orbital.

Such results are, of course, preliminary but can serve as guides for more accurate surface and tip models. In particular, we are currently using first-row transition metals as surface and tip models. Simple atomic and molecular adsorbates can then be bonded to the "surface" in order to examine the perturbations to $T_{\mu\nu}$ caused by the adsorbate. The possible increase in electronic coupling between the initial and final states due to the presence of an intervening medium has been discussed previously [34, 35].

There are several ways to assess the importance of effects such as the possible overadjustment of the remaining electronic cloud upon electron transfer on the calculated $T_{\mu\nu}$ in the present model. First, using single-atom surface and tip models, results from calculations of $T_{\mu\nu}$ could be compared using systems having either frozen or relaxed cores. The present results used relaxed cores; that is, the cores were able to respond to the presence or absence of the extra electron at a center. The frozen core results would give an indication of the extent of the effects of such relaxation on $T_{\mu\nu}$.

Another method of assessing these effects is to increase the cluster size. It is reasonable to assume that such problems will be greatest for the single-atom surface and tip models and will decrease as the cluster size increases. One area of interest which can be explored through the use of a variety of cluster sizes is the sensitivity of $T_{\mu\nu}$ to the tip size and shape. Models of proposed tip shapes can be easily tested and the results compared with single-atom tips. While such tip-shape effects have been considered previously in a general fashion [10, 19, 22, 23], apparently no molecular models have been examined yet.

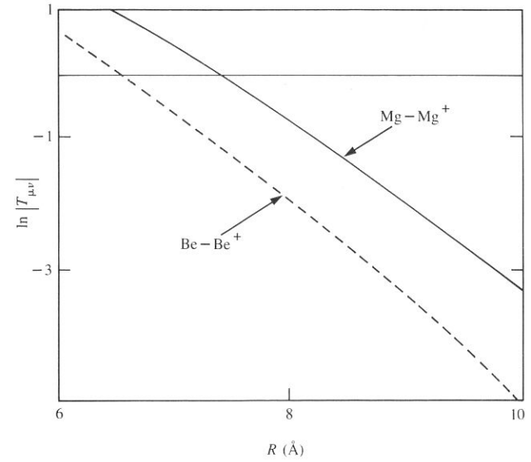

Figure 6

Plot of $\ln|T_{\mu\nu}|$ as a function of center-to-center separation distance for the atomic pairs $Be–Be^+$ and $Mg–Mg^+$. The values of $T_{\mu\nu}$ are in millihartrees, the separation distances in Å.

• *Systems to be studied*

Our long-term objective for research using the STM is the study of systems of chemical interest. These studies will focus on such issues as the nature of the surface adsorbate interaction, chemical processes on surfaces, and the structure of the wave functions of adsorbates ranging in size from single atoms to macromolecules.

Benzene will probably be one of the first molecular species that we will study. Benzene chemisorbs to atomically flat clean metal surfaces by interaction of the ring π^* orbitals with the appropriate metal surface orbitals. The C_6 ring is generally parallel to the surface plane [36, 37], but the position of the hydrogen atoms cannot be established from available spectroscopic data. Chemical studies suggest that the hydrogen atoms may lie further from the crystal plane than the C_6 ring [38, 39]. STM may provide a means of probing this structure. The various intermediates in benzene hydrogenation [40] may be investigated as well.

Another simple system which we will likely study with the STM is the coordination of pyridine to transition metal surfaces. Pyridine is believed to bind to Pt(111) and (100) through the nitrogen atom on the basis of work-function

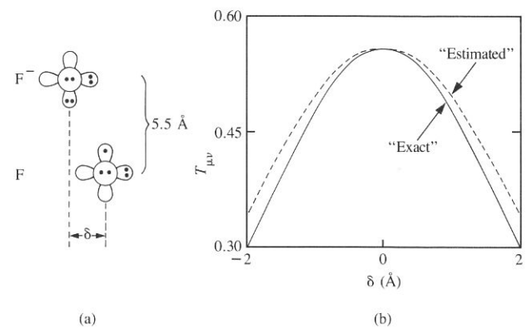

Figure 7

(a) Schematic description of the orientations between the two fluorine atoms for which $T_{\mu\nu}$ was calculated. (b) $T_{\mu\nu}$ (millihartrees) vs. (Å) for the "Exact" and "Estimated" calculations described in the text.

measurements [41, 42]. Near-edge absorption studies have established that chemisorbed pyridine on Pt(111) is prependicular to the surface plane for coverages above 0.1 monolayers [43]. However, recent photoemission data indicate that either the nitrogen lone pair or the aromatic cloud, or both, may be involved in the bonding of pyridine to Pd(111) [44], Ir(111) [45], Cu(110) [46], and Ag(111) [47]. The STM should yield useful information on the structure of surface-bound pyridine.

Various porphyrins would appear to be ideal candidates for early studies of larger molecules. For example, the metal-phthalocyanines are extremely stable, planar species of well-known molecular and electronic structure. They can be readily obtained containing metal atoms such as copper, and can be sublimed onto surfaces at moderate temperatures in high vacuum. When larger metal atoms such as vanadium are incorporated in these structures, the metal atom no longer lies in the plane of the conjugated structure. These structural variations should be readily observable by STM.

Acknowledgments

The support of the Office of Naval Research (Contract No. N00014-84-K-0638), the Shell Company Foundation Inc., and the President's Fund of Caltech are gratefully acknowledged.

References and note

1. Shuk Y. Tong, *Phys. Today* **37,** 50 (August 1984).
2. G. Binnig, H. Rohrer, Ch. Gerber, and E. Weibel, *Appl. Phys. Lett.* **40,** 178 (1982).
3. G. Binnig, H. Rohrer, Ch. Gerber, and E. Weibel, *Phys. Rev. Lett.* **49,** 57 (1982).
4. G. Binnig and H. Rohrer, *Helv. Phys. Acta* **55,** 726 (1982).
5. G. Binnig and H. Rohrer, *Surf. Sci.* **126,** 236 (1983).
6. G. Binnig, H. Rohrer, Ch. Gerber, and E. Weibel, *Phys. Rev. Lett.* **50,** 120 (1983).
7. A. Baratoff, G. Binnig, and H. Rohrer, *J. Vac. Sci. Technol. B* **1,** 703 (1983).
8. G. Binnig, H. Rohrer, Ch. Gerber, and E. Weibel, *Surf. Sci.* **131,** 379 (1983).
9. A. Baró, G. Binnig, H. Rohrer, Ch. Gerber, E. Stoll, A. Baratoff, and F. Salvan, *Phys. Rev. Lett.* **52,** 1304 (1984).
10. J. Pendry, *Low Energy Electron Diffraction*, Academic Press, London, 1974.
11. C. Carrol and J. May, *Surf. Sci.* **29,** 60 and 85 (1972).
12. J. Simmons, *J. Appl. Phys.* **34,** 1793 (1963).
13. J. Golovchenko, AT&T Laboratories, Holmdel, NJ, private communication.
14. C. Gerber, IBM Research Division, Zurich, Switzerland, private communication.
15. S. Elrod, A. de Lozanne, and C. Quate, *Appl. Phys. Lett.* **45,** 1240 (1984), and private communication.
16. T. H. Upton and W. A. Goddard III, *Phys. Rev. Lett.* **42,** 472 (1979).
17. P. E. M. Siegbahn, M. R. A. Blomberg, and C. W. Bauschlicher, Jr., *J. Chem. Phys.* **81,** 2103 (1984).
18. N. Garcia, C. Ocal, and F. Flores, *Phys. Rev. Lett.* **50,** 2002 (1983).
19. G. Binnig, N. Garcia, H. Rohrer, J. M. Soler, and F. Flores, *Phys. Rev. B* **30,** 4816 (1984).
20. E. Stoll, A. Baratoff, A. Selloni, and P. Carnevali, *J. Phys. C* **17,** 3073 (1984).
21. A. Baratoff, *Europhys. Conf. Abstr.* **76,** 364 (1983).
22. J. Tersoff and D. R. Hamann, *Phys. Rev. Lett.* **50,** 1998 (1983).
23. J. Tersoff and D. R. Hamann, *Phys. Rev. B* **31,** 805 (1985).
24. N. D. Lang, *Phys. Rev. Lett.* **55,** 230 (1985).
25. J. Bardeen, *Phys. Rev. Lett.* **6,** 57 (1961).
26. N. R. Kestner, J. Logan, and J. Jortner, *J. Phys. Chem.* **78,** 2148 (1974).
27. R. J. Cave, Ph.D. Thesis, California Institute of Technology, Pasadena, 1986, Ch. 1.
28. M. D. Newton, *Int. J. Quantum Chem.: Quantum Chem. Symp.* **14,** 363 (1980).
29. J. Logan and M. D. Newton, *J. Chem. Phys.* **78,** 4086 (1983).
30. B. L. Tembe, H. L. Friedman, and M. D. Newton, *J. Chem. Phys.* **76,** 1490 (1982).
31. A. F. Voter, Ph.D. Thesis, California Institute of Technology, Pasadena, 1983.
32. The basis sets used to describe each F-atom were a standard (9s, 5p/3s, 2p) Huzinaga/Dunning basis set augmented with a set of negative ion functions (s exponent = 0.112, p exponent = 0.076) and a set of diffuse Rydberg functions (s exponent = 0.036, p exponent = 0.029, d exponent = 0.015). To describe Cl and Mg, the Ne core in each case was replaced by an SHC effective potential of Rappe, Smedley, and Goddard [*J. Phys. Chem.* **85,** 1662 (1981)]. The valence basis set for Cl comprised a double zeta set of s and p functions, optimized for the effective potential used, a set of d polarization functions (exponent = 0.6) and a set of p negative ion functions (exponent = 0.049). For Mg, a double zeta valence set appropriate to the SHC effective potential was used. Finally, the basis set used in the Be calculations was the standard (9s, 5p/3s, 2p) Huzinaga/Dunning set.
33. A. Szabo and N. R. Ostlund, *Modern Quantum Chemistry*, Macmillan Publishing Co., New York, 1982, p. 127.
34. J. Halpern and L. E. Orgel, *Discuss. Faraday Soc.* **29,** 32 (1960).
35. H. M. McConnell, *J. Chem. Phys.* **35,** 508 (1961).
36. S. Lehwald, H. Ibach, and J. Demuth, *Surf. Sci.* **78,** 577 (1978).
37. J. Bertolini and J. Rousseau, *Surf. Sci.* **89,** 467 (1979).
38. M. Tsai and E. Muetterties, *J. Amer. Chem. Soc.* **104,** 2534 (1982).
39. M. Tsai and E. Muetterties, *J. Phys. Chem.* **86,** 5067 (1982).
40. M. Tsai, C. Friend, and E. Muetterties, *J. Amer. Chem. Soc.* **104,** 2539 (1982).
41. J. Gland and G. Somorjai, *Surf. Sci.* **38,** 157 (1973).
42. J. Gland and G. Somorjai, *Adv. Coll. Interface Sci.* **5,** 205 (1976).
43. A. Johnson, E. Muetterties, and J. Stöhr, *J. Amer. Chem. Soc.* **105,** 7183 (1983).
44. F. Netzer and J. Mack, *Chem. Phys. Lett.* **95,** 492 (1983).
45. F. Netzer and J. Mack, *J. Chem. Phys.* **79,** 1017 (1983).
46. B. Bandy, D. Lloyd, and N. Richardson, *Surf. Sci.* **89,** 344 (1979).
47. J. Demuth, K. Christmann, and P. Sanda, *Chem. Phys. Lett.* **76,** 201 (1980).

Received August 8, 1985; accepted for publication November 6, 1985

Paul West *Aerojet Electro Systems Co., Surface Science Laboratory, Azusa, California 91702.* Dr. West is a senior staff member at Aerojet Electrosystems. Prior to joining Aerojet, he was a Postdoctoral Fellow at the California Institute of Technology, Pasadena, for the academic year 1983–84. While at Caltech, he designed and constructed the scanning tunneling microscope. He received his Ph.D. in physical chemistry from Wesleyan University, Middletown, Connecticut, in 1983. His research interests include operation and application of laser and dye laser systems, cryogenic techniques, and computer programming.

John Kramar *California Institute of Technology, Department of Chemistry, Pasadena, California 91125.* Mr. Kramar is a graduate student in chemistry at Caltech. He is currently involved in the design and construction of a second-generation scanning tunneling microscope which will include a sample-preparation chamber and improved vibrational stability.

David V. Baxter *McGill University, Montreal, Quebec, Canada.* Dr. Baxter is a National Science and Engineering Research Council Postdoctoral Fellow doing research in the structural and electrical properties of noncrystalline metallic alloys using X-ray absorption, X-ray diffraction, and low-temperature transport measurements, as well as collaborating with Dr. Robert Cave of the California Institute of Technology, Pasadena, on the theory of scanning tunneling microscopy. Prior to this, he was a Postdoctoral Fellow at the California Institute of Technology, where he received his Ph.D. in applied physics in 1984. Dr. Baxter is a member of the American Physical Society.

Robert J. Cave *California Institute of Technology, Department of Chemistry, Pasadena, California 91125.* Dr. Cave is a Research Associate in Chemistry at Caltech; he joined the Baldeschwieler group in 1985. He received his Ph.D. at Caltech and from 1979 to 1985 was a National Science Foundation Predoctoral Fellow. His research interests include solution electron transfer theory and theoretical investigations of atom-molecule collision dynamics.

John D. Baldeschwieler *California Institute of Technology, Division of Chemistry and Chemical Engineering, Pasadena, California 91125.* Dr. Baldeschwieler is Professor of Chemistry at Caltech. He received his Bachelor of Chemical Engineering degree from Cornell University, Ithaca, New York, in 1956, and his Ph.D. in physical chemistry from the University of California, Berkeley, in 1959. The following year he joined the faculty of Harvard University, Cambridge, Massachusetts, as Instructor and Assistant Professor of Chemistry. He moved to Stanford University in 1965 as Associate Professor and Professor of Chemistry. Dr. Baldeschwieler served as Deputy Director of the Office of Science and Technology in the Executive Office of the President from 1971 through 1973. He then joined the faculty of Caltech as Professor and Chairman of the Division of Chemistry and Chemical Engineering. He is best known for his work in developing nuclear magnetic double resonance techniques, ion cyclotron resonance spectroscopy, and perturbed angular correlation spectroscopy. His research interests also include applications of these methods to biological systems. Dr. Baldeschwieler has served on numerous national committees and is a member of the American Philosophical Society and the National Academy of Sciences.